

Supplemental material

Knipfer et al., <https://doi.org/10.1084/jem.20182111>

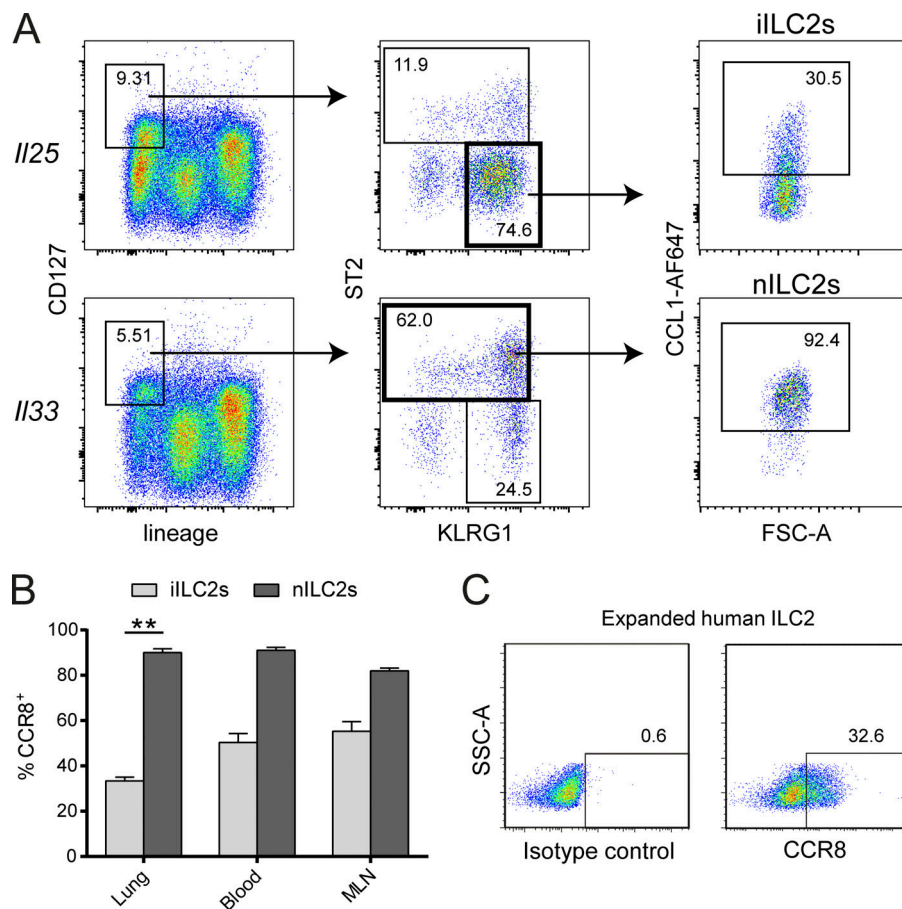


Figure S1. **Flow cytometric analyses of CCR8 on ILC2s.** (A) Gating strategy for iILC2s (treatment with *Il25* vectors) and nILC2s (treatment with *Il33* vectors) in mouse lung cells after treatment with *Il25* or *Il33* DNA vectors. Debris and doublets were excluded and a lymphocyte gate set. iILC2s (Lin⁻CD127⁺KLRG1^{hi}ST2⁻) and nILC2s (Lin⁻CD127⁺KLRG1^{int}ST2⁺) were analyzed for CCR8 expression (CCL1-AF657). (B) CCR8 expression was determined on iILC2s and nILC2s in lungs, peripheral blood, and mesenteric lymph nodes (MLNs). Results in A and B are representative for one out of two independent experiments with two to five mice in each experimental group. (C) Sorted and in vitro-cultured human ILC2s were analyzed for CCR8 surface expression. Representative plots of one out of three independent sorting experiments are shown. Data represent mean ± SEM. **, P ≤ 0.01 by Mann-Whitney U tests. FSC-A, forward scatter-area; SSC-A, side scatter-area.

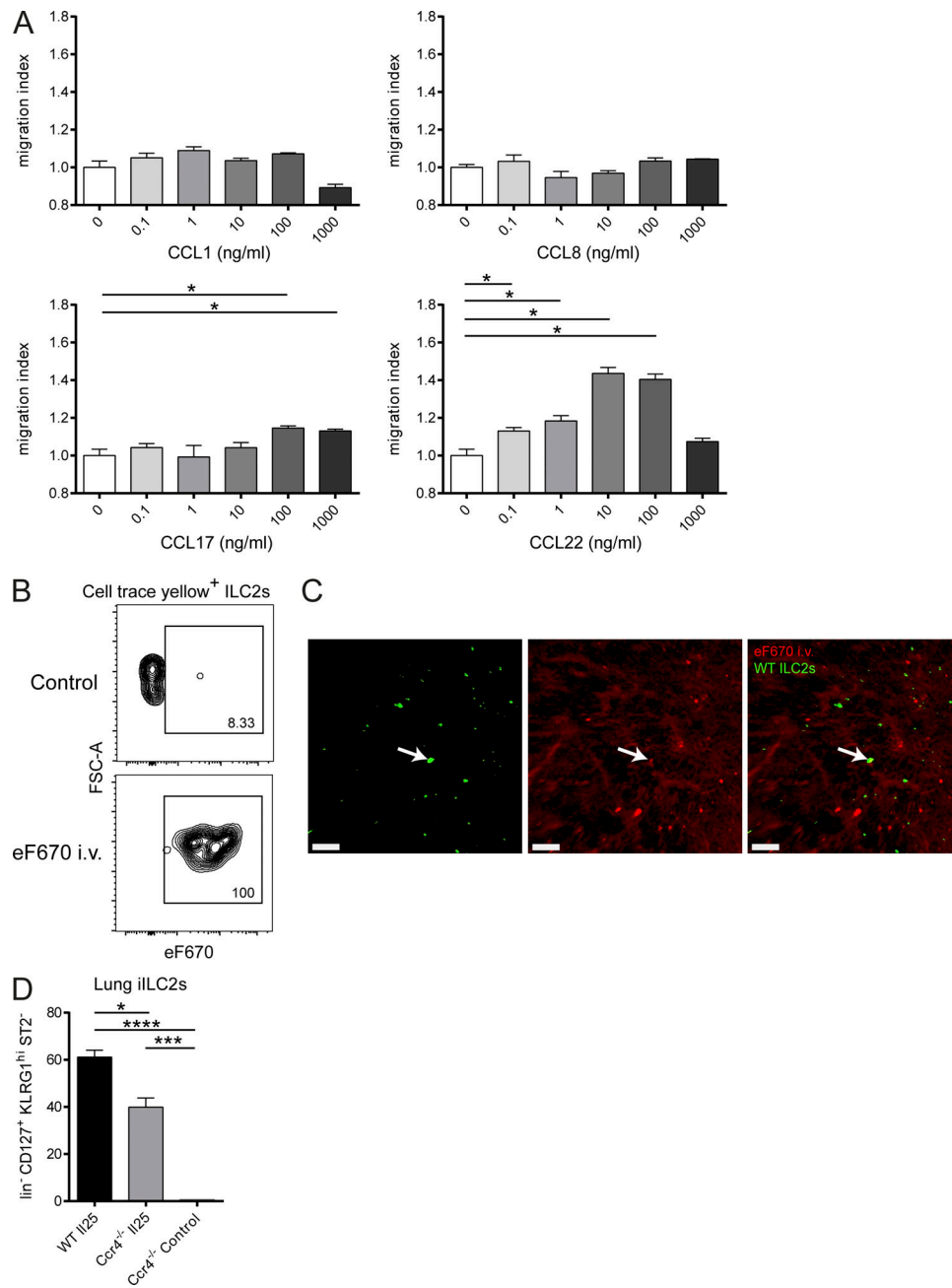


Figure S2. **Analysis of the in vitro and in vivo migratory behavior of ILC2s.** (A) Chemotaxis assays using transwell inserts were performed with in vitro-expanded WT ILC2s against CCL1, CCL8, CCL17, and CCL22 gradients at the indicated concentrations. Experimental groups consist of at least three technical replicates. (B and C) To distinguish vascular from extravasated ILC2s in lung homing experiments, Cell trace eF670 dye was injected i.v. 10 min before lung harvesting. (B) Complete staining of vascular transferred ILC2s was confirmed by flow cytometry of peripheral blood cells. Therefore, transferred ILC2s (CellTrace yellow⁺) were analyzed for eF670 staining and compared with mice that did not receive eF670 i.v. (control). (C) Light-sheet microscopy of lungs showing transferred ILC2s (left picture, green) and eF670 staining (middle picture, red). The arrows in the overlay picture (right picture) indicate a double-stained cell. Scale bars are 200 μ m. Graphs in B–D show one representative sample out of two independently performed experiments. (D) To investigate the role of CCR4 for lung accumulation of iILC2s, WT and *Ccr4*^{-/-} mice were treated with *Il25* vectors or left untreated (control) for 5 d, and iILC2s (*lin*⁻ CD127⁺ KLRG1^{hi} ST2⁻) in lungs were enumerated by flow cytometry. The graph shows one representative experiment out of two independently performed experiments with two to five animals in one experimental group. One-way ANOVA was applied. Data represent mean \pm SEM. *, $P \leq 0.05$; ***, $P \leq 0.001$; ****, $P \leq 0.0001$ by Mann–Whitney *U* tests or, if indicated, one-way ANOVA.

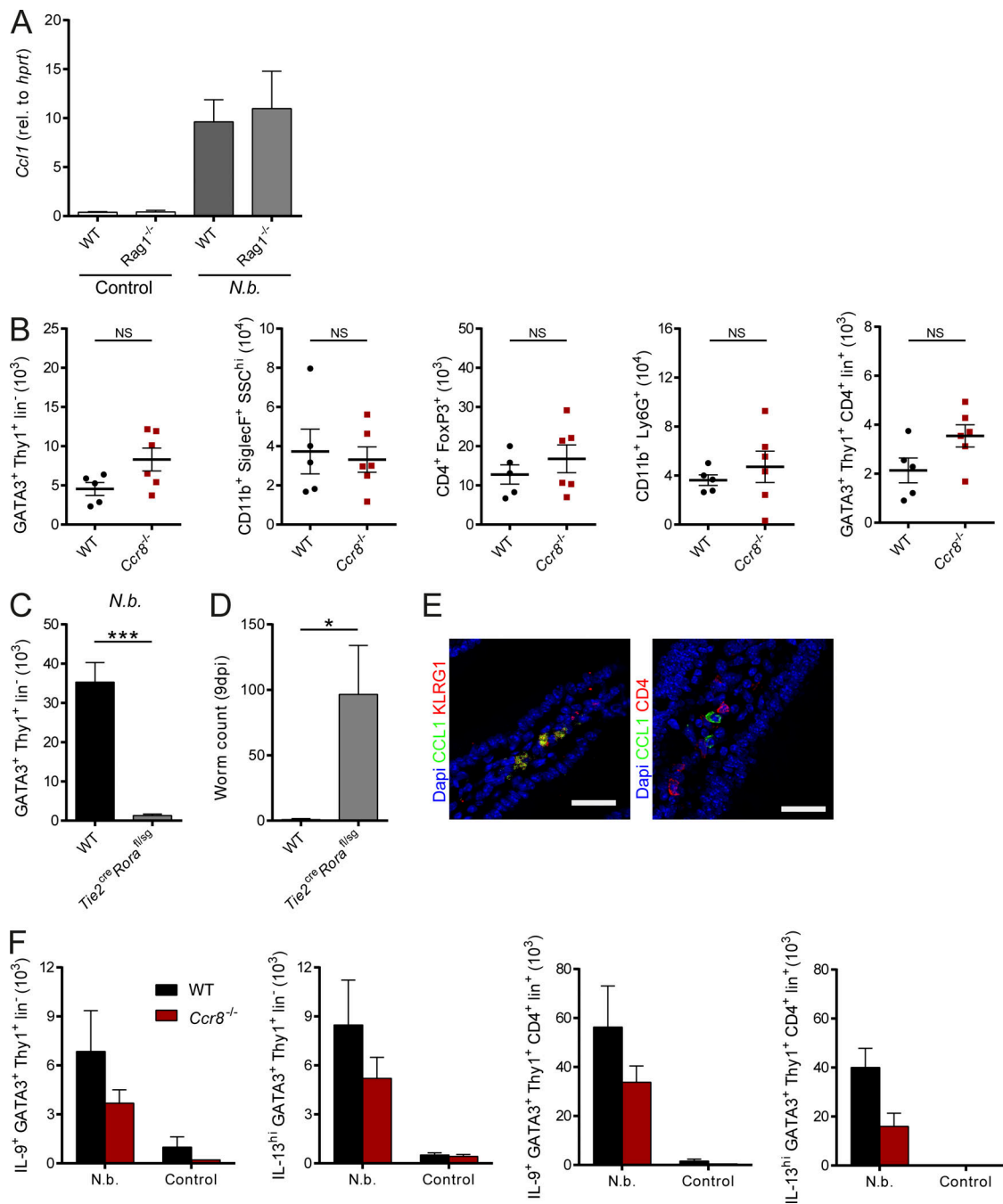


Figure S3. **Analysis of immune cell populations in naive and *N. brasiliensis*-infected mice.** (A) *Rag1*^{-/-} and C57BL/6 mice were infected with *N. brasiliensis* (*N.b.*) or left untreated and analyzed after 9 d for *Ccl1* expression in lungs by qPCR. (B) Flow cytometric analysis of immune cell populations in lungs of naive WT and *Ccr8*^{-/-} mice. (C and D) *Tie2*^{cre}*Rora*^{fl/sf} and littermate control mice (WT) were infected with *N. brasiliensis* and analyzed after 9 d. (C) ILC2 (GATA3⁺Thy1⁺Lin⁻) numbers per lung were determined by flow cytometry. (D) Adult worm counts in small intestinal tissues were determined. (E) Small intestinal tissue sections of C57BL/6 WT mice infected with *N. brasiliensis* were stained with DAPI (blue), anti-CCL1 (green), and anti-KLRG1 (red, left), or anti-CD4 (red, right) antibodies and analyzed by confocal microscopy. Scale bars are 30 μm. Pictures show results of one representative animal. (F) Mice were infected with *N. brasiliensis* or left untreated (control) and analyzed after 9 d for IL-9⁺ or IL-13^{hi} ILC2s or Th2 cells. All graphs show data of one representative experiment out of two independently performed experiments with at least three mice in each experimental group. Data represent mean ± SEM. P > 0.05; *, P ≤ 0.05; ***, P ≤ 0.001 by Mann-Whitney *U* tests.

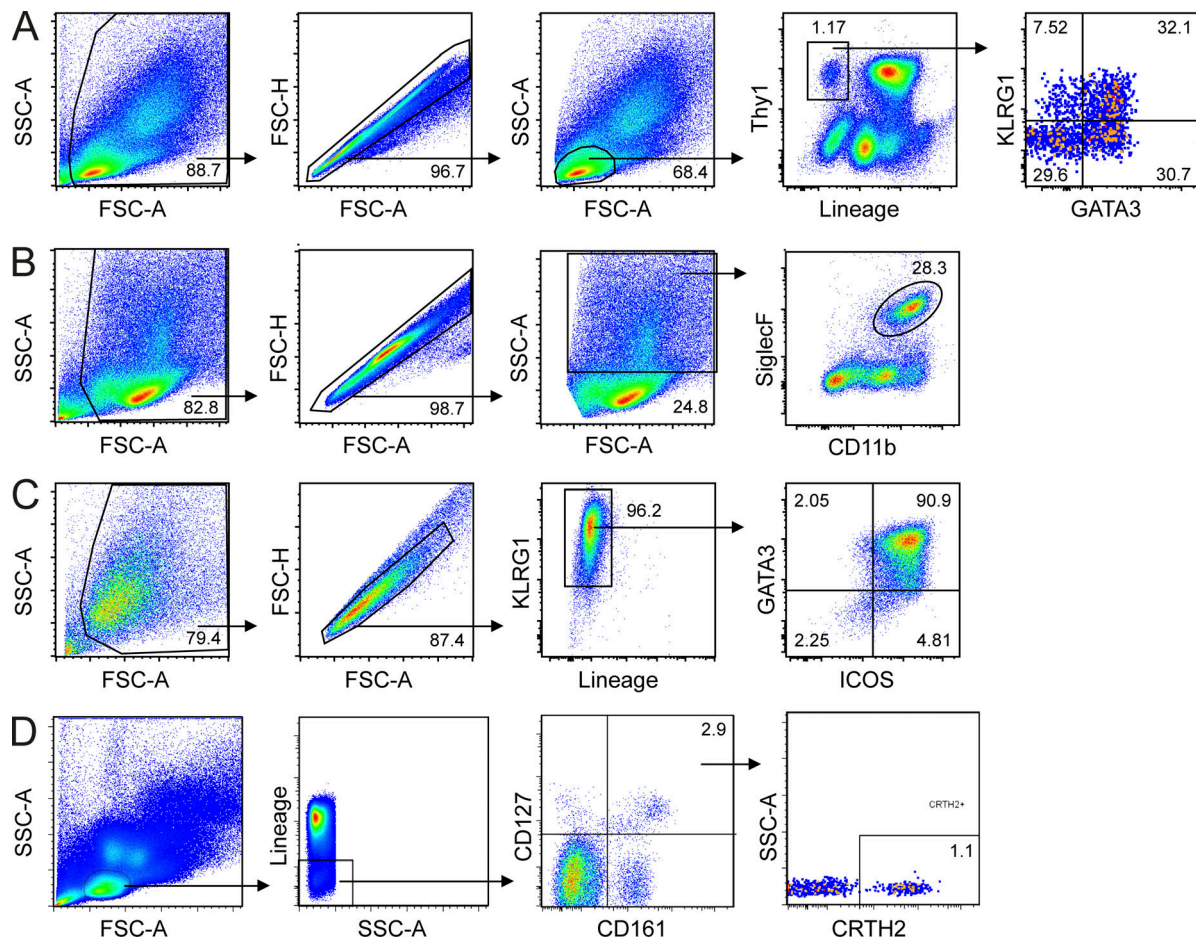
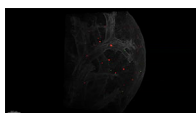


Figure S4. **Flow cytometry gating strategies of ILC2s.** (A) Gating strategy for ILC2s in *N. brasiliensis*-challenged lungs after 9 d. Debris and doublets were excluded and lymphocytes selected. ILCs (Lin⁻Thy1⁺) were analyzed for GATA3 and KLRG1 expression. (B) Gating strategy for eosinophils in lungs of *N. brasiliensis*-infected mice. Eosinophils were defined as CD11b⁺SiglecF⁺SSC^{hi} cells. (C) Characterization of in vitro-expanded ILC2s 9 d after sorting. Debris and doublets were excluded, and Lin⁻KLRG1⁺ ILC2s were analyzed for Gata3 and ICOS expression. (D) Gating strategy for analysis and sorting of human ILC2s in freshly isolated human PBMCs. Within lineage⁻ lymphocytic cells, CD127⁺CD161⁺ cells were analyzed for CRTH2 expression. All results are representative flow cytometry plots of one WT animal (A–C) or donor (D) in the respective experiment. FSC-A, forward scatter–area; FSC-H, forward scatter–height; SSC-A, side scatter–area.



Video 1. **CCR4 mediates ILC2 migration in in vivo lung homing experiments.** To investigate ILC2 lung homing, WT mice were pretreated with papain, and 10⁶ fluorescent-labeled WT (red) and *Ccr4*^{-/-} (green) ILC2s in a 50:50 mix were adoptively transferred by i.v. injection. 24 h later, lungs were collected, processed, and analyzed by light-sheet microscopy. Images were acquired with a 25× zoom factor. Playback rate is 10 frames per second. Snapshots of this video are provided in Fig. 2 D.